Title

White matter disruption in moderate/severe pediatric traumatic brain injury: Advanced tract-based analyses

Authors

Dennis, Emily L
Jin, Yan
Villalon-Reina, Julio E
et al.

Publication Date

2015

DOI

10.1016/j.nicl.2015.02.002

Peer reviewed

FIBER TRACKING IN TRAUMATIC BRAIN INJURY: COMPARISON OF 7 TRACTOGRAPHY ALGORITHMS

Emily L. Dennis[1], Gautam Prasad[1], Madelaine Daianu[1], Liang Zhan[1], Claudia Kernan[2], Talin Babikian[2], Richard Mink[3], Christopher Babbitt[4], Jeffrey Johnson[5], Christopher C. Giza[6], Robert F. Asarnow[2,7], Paul M. Thompson[1,2,8]

[1]Imaging Genetics Center, USC Keck School of Medicine, Los Angeles, CA, USA; [2]Department of Psychiatry and Biobehavioral Sciences, Semel Institute for Neuroscience and Human Behavior, UCLA, Los Angeles, CA, USA; [3]Harbor-UCLA Medical Center and Los Angeles BioMedical Research Institute, Department of Pediatrics, Torrance, CA, USA; [4]Miller Children's Hospital, Long Beach, CA, USA; [5]LAC+USC Medical Center, Department of Pediatrics, Los Angeles, CA, USA; [6]UCLA Brain Injury Research Center, Dept of Neurosurgery and Division of Pediatric Neurology, Mattel Children's Hospital, Los Angeles, CA, USA; [7]Department of Psychology, UCLA, Los Angeles, CA, USA; [8]Departments of Neurology, Pediatrics, Psychiatry, Radiology, Engineering, and Ophthalmology, USC;

ABSTRACT

Traumatic brain injury (TBI) is the leading cause of death and disability in children. Among the many neurological disruptions that follow an injury, damage to the white matter is among the most common and long-lasting. Diffusion weighted imaging methods are uniquely sensitive to this disruption. Even so, traumatic injury disrupts the brain anatomy we aim to study, complicating the analysis of brain integrity and connectivity, which are typically analyzed using tractography methods optimized for analyzing normal healthy brains. To understand which fiber tracking methods show promise for analysis of TBI, we tested 7 different tractography algorithms for their accuracy and ability to detect group differences between children with TBI and matched controls. We also tested which elements (corresponding to neural bundles) in the resulting connectivity matrices provided the most useful information for accurately detecting group differences.

Index Terms— High angular resolution diffusion imaging (HARDI), traumatic brain injury, tractography, connectivity

1. INTRODUCTION

Traumatic brain injury (TBI) can cause extensive white matter (WM) damage that can be long-lasting and far reaching in its associated impairments. Diffuse axonal injury (DAI) is partly responsible, and is frequently detectable in the corpus callosum, brain stem, gray-white matter junctions, and the parasagittal white matter. While DAI can only be definitively diagnosed *post mortem*, diffusion weighted imaging (DWI) has shown great potential in detecting these disruptions.

Disruptions in WM integrity caused by TBI are observable as decreased FA (fractional anisotropy) and increased MD (mean diffusivity), indicating myelin disruption [1]. These FA dropouts can make advanced analyses such as tractography difficult, as tract-propagation methods may stop in regions where the fractional anisotropy is abnormally low. As tractography algorithms vary in the equations and models they use reconstruct tracts, they may also vary in their success in tracking fibers through disrupted regions. To investigate how different fiber tracking methods perform on scans from children with TBI, we tested 7 different tractography algorithms to see how sensitive the resulting connectivity matrices are in differentiating between our groups.

In the developing brain, TBI is especially disruptive. In animal studies, TBI during development can decrease experience-dependent plasticity - a key process for brain maturation and development [2]. TBI during development can delay or alter the maturation of WM tracts. Even today, little is known about how TBI affects developing brains, what course recovery may follow, and what interventions may assist in the process.

2. METHODS

2.1. Subjects and Image Acquisition

TBI participants were recruited from 4 Pediatric Intensive Care Units (PICUs) at Level 1 Trauma Centers in Los Angeles County. Healthy controls, matched for age, sex, and educational level, were recruited from the community through flyers, magazines, and school postings. Participants were studied in the chronic phase (13-19 months post-injury). We included 13 TBI participants (4 female) and 13 controls, matched for age and sex. *Inclusion criteria*: non penetrating moderate-severe TBI (intake or post-resuscitation GCS score between 3 and 12), 8-19 years old, right handed, normal vision, English proficiency. *Exclusion criteria*: history of neurological illness or injury, motor deficits or metal implant preventing safe MRI scanning, history of psychosis, ADHD, Tourette's, learning disability, mental retardation, autism, or substance abuse.

Participants were scanned using 3T MRI (Siemens Trio) with whole-brain anatomical and 66-gradient diffusion imaging. Diffusion-weighted images (DWI) were acquired with the following acquisition parameters: GRAPPA mode;

acceleration factor PE=2; TR/TE=9500/87 ms; FOV=256x256mm; isotropic voxel size=2 mm. 66 images were collected per subject: 2 b_0 and 64 diffusion-weighted images (b=1000 s/mm^2).

2.2 Data Preprocessing and Cortical Extraction

Non-brain regions were automatically removed from a b0 image from the DWI volume using the *bet* function in the FSL toolbox (http://fsl.fmrib.ox.ac.uk). Brainsuite was used for the T1-weighted images (http://brainsuite.org); these brain extractions were refined by a neuroanatomical expert. DWI volumes were corrected for eddy current distortion using FSL's *eddy_correct* function. All T1-weighted scans were linearly aligned to a common template using 9 DOF. Averaged b0 maps were elastically registered to the structural scan using a mutual information cost function to compensate for EPI-induced susceptibility artifacts. Based on these DWIs, whole brain tractography was conducted using 7 different deterministic and probabilistic tracking algorithms.

34 cortical labels per hemisphere [3] were automatically extracted from aligned T1-weighted structural MRI scans using FreeSurfer (http://surfer.nmr.mgh.harvard.edu/), aligned to the T1-weighted images, and downsampled using nearest neighbor interpolation to the space of the DWIs. To ensure tracts would intersect cortical label boundaries, labels were dilated with an isotropic box kernel of width 5 voxels. We created 7 68x68 connectivity matrices for each subject using each tractography method separately. Each element of the matrix described the number of fibers that passed through each pair of cortical labels - or regions of interest (ROIs).

2.3 Tractography

We tested seven different tractography methods, including three tensor-based deterministic algorithms: FACT [4], 2nd order Runge-Kutta (RK2) [5], and tensorline (TL) [6], and two deterministic tractography algorithms based on the 4th order spherical harmonic derived orientation distribution functions (ODFs) – FACT and RK2. We also tested the Hough voting method [7], which is based on ODFs represented by 4th order spherical harmonics, and the Probabilistic Index of Connectivity (PICo) [8], based on ODFs represented by 6th order spherical harmonics. For the Hough method, tract reconstruction was constrained to 10,000 fibers.

The five deterministic methods were run with Diffusion Toolkit (http://trackvis.org/dtk/). Fiber tracking was restricted to regions with fractional anisotropy (FA) $\geq$ 0.2 to avoid gray matter and cerebrospinal fluid; fiber paths were stopped if the fiber direction encountered a sharp turn (with a critical angle threshold $\geq$ 30°). Recent reports have suggested that fiber angles as sharp as 90° may be biologically plausible [9], but such a large threshold can also allow for large numbers of false positive fibers.

The Hough method was performed using an optimized implementation relying on a lookup table and described previously [7,10]. Voxels with an FA $\geq$ 0.2 were probabilistically seeded, and 10,000 fibers were reconstructed. PICo was conducted with Camino (http://cmic.cs.ucl.ac.uk/camino/). Voxels with an FA $\geq$ 0.2 seeded, ODFs were estimated using 6th order spherical harmonics and a maximum of 3 local ODF maxima to be detected. The fiber turning angle threshold was set to 30°/voxel, and tracing was stopped at any voxels with an FA < 0.2.

2.4 Support Vector Machine (SVM) Classification

To automatically identify connectivity patterns in TBI from normal development we used the machine learning classifier support vector machines (SVMs) [11]. The method works by learning the parameters of a hyperplane that optimally separates the two groups of points.

Formally, we can let $x_i \in R^d$ represent the features that are derived from all the connections organized in the connectivity matrix, where in our data d is 68*68 = 4,624 in dimension and since our matrices are symmetric this number can drop to 2,278 unique features. We let $Y_i = \pm 1$ represent the group label of each subject with -1 and 1 representing TBI and control respectively. We compute a hyperplane as:

$$\langle w,x \rangle + b = 0,$$

choosing $w \in R^d$ such that it separates the maximal number of points possible. The hyperplane can be posed as the following L2-norm problem:

$$\arg\min_{w,b,v} \left(\frac{1}{2} \langle w,w \rangle + D \sum_i v_i^2 \right),$$

such that

$$y_i(\langle w,x_i \rangle + b) \geq 1 - v_i,$$
$$v_i \geq 0$$

where we let v_i be slack variables and D controls a penalty parameter. This formulation is necessary because in many real applications the hyperplane is not able to completely separate the two classes and we need to provide additional flexibility to the method.

To evaluate the performance of the classification algorithm we used 10 times repeated stratified 10-fold cross-validation [12,13]. This approach has been shown to balance the amount of bias and variance in its estimate in both synthetic and real data. In each repetition of cross-validation we cataloged the accuracy, specificity, and sensitivity as the metrics for performance.

In addition to performance metrics, we computed a ranking of features in each of the classification problems. This ranking was derived using a standard technique [14] that evaluates each feature's relationship to the optimal hyperplane. These values are quantified by $|w|$ in the above equations and by sorting these values in decreasing order we compute a ranking from most important to least important feature. The interpretation of features with high weights is that they have a greater influence on the decision of the

boundary represented in the hyperplane. We use the collection of weights to understand what connections in the network are driving the classification rule and are being sampled effectively in a certain tractography algorithm.

3. RESULTS

3.1. Comparing Tractography Algorithm Outputs

Descriptive statistics for the 7 tractography algorithm outputs for the TBI and control groups are shown in **Figures 1** and **2**. **Figure 1** displays the number of tracts reconstructed, while **Figure 2** displays the maximum length of the tracts reconstructed.

The number of tracts reconstructed was similar across the 5 deterministic methods. As expected, PICo (Camino) generated many more streamlines in the brain than the other methods, and the Hough method was constrained to generate only 10000 fibers. Between TBI and controls, there were no detectable differences in the number of tracts or maximum length of tracts reconstructed.

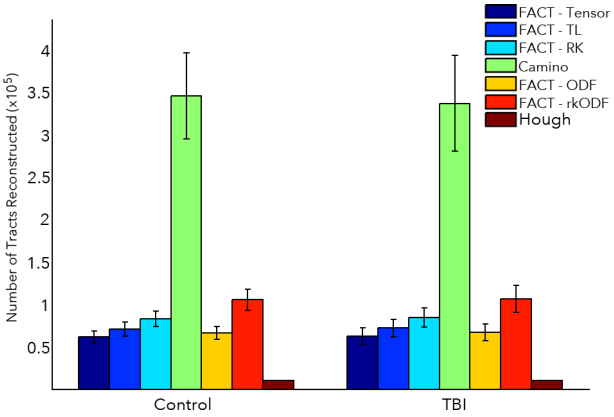

Figure 1. Number of tracts reconstructed across all 7 tractography algorithms, across control and TBI subjects. For the Hough method, tract reconstruction was constrained to 10,000 fibers.

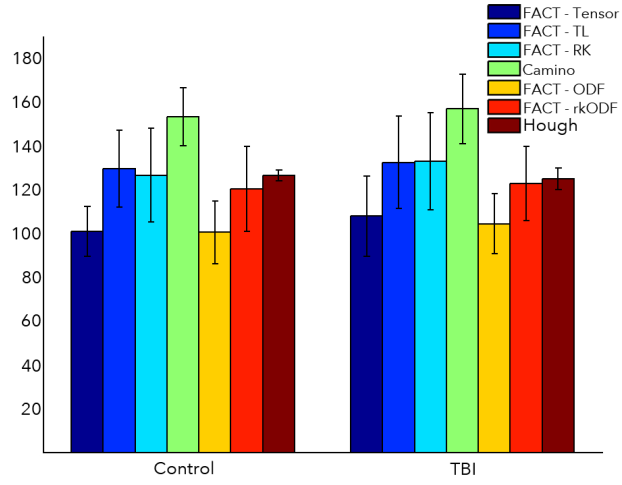

Figure 2. Maximum length of tracts reconstructed across all 7 tractography algorithms, across control and TBI subjects.

3.2. SVM Accuracy of Connectivity Matrices

To rank the tractography algorithms, we compared the accuracies of the SVM associated with the connectivity matrices. Results are shown in **Table 1**.

	Accuracy	Specificity	Sensitivity
FACT - Tensor	0.5536	0.7714	0.3357
FACT - TL	0.5964	0.6714	0.5214
FACT - RK	0.5821	0.65	0.5143
Camino	0.4357	0.3857	0.4857
FACT - ODF	0.55	0.5857	0.5143
FACT - rkODF	0.4643	0.5643	0.3643
Hough	0.5179	0.55	0.4857

Table 1. SVM classification accuracy, specificity, and sensitivity across the 7 tractography algorithms tested.

From these analyses, the FACT – TL tractography algorithm had the best accuracy in our dataset, with FACT – RK close behind.

3.3. Most Robust Elements in Connectivity Matrix

After we determined that the FACT - TL tractography algorithm was the most accurate for group classification, we further investigated which connections contributed most. **Figure 3** displays the connections that ranked in the top 5% in classification weight (of the non-zero matrix elements).

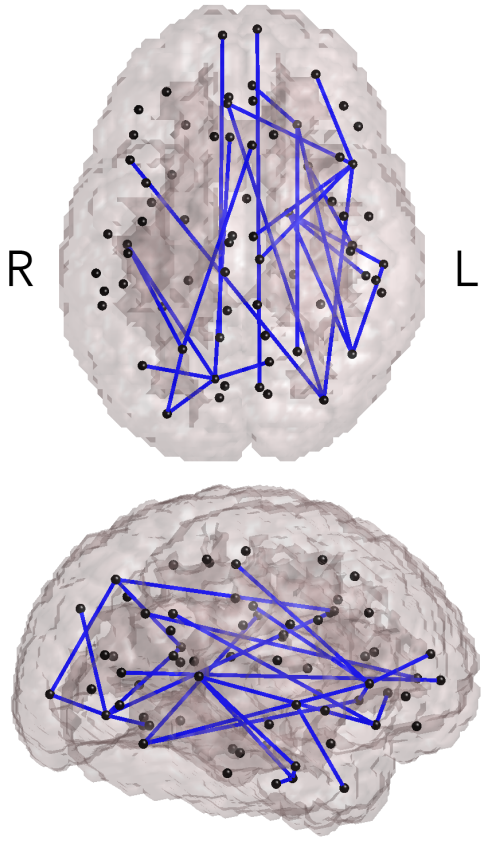

Figure 3. Connections with the highest weight in the classification. The top 5% of connections (out of non-zero matrix elements) are shown in blue, with all ROIs indicated by black spheres. Left in image is right in brain.

The most robust elements in the connectivity matrices fed into the SVM classifier included connections spanning all lobes, both interhemispheric and intrahemispheric. Of these, connections terminating in the left hemisphere were more numerous than those terminating in the right. There were a number of long-range, anterior-posterior connections included in these most robust connections.

4. DISCUSSION

TBI causes widespread damage to WM integrity, but there has been little comprehensive comparison of fiber tracking methods that may be used to examine this damage. Here we compared 7 tractography algorithms, testing which was most accurate in separating TBI patients from controls. When connectivity matrices resulting from these different algorithms were entered into SVM classification schemes, FACT – TL (tensorline) emerged with the greatest accuracy. In healthy individuals, higher resolution analyses using probabilistic methods and ODFs instead of tensors typically result in more robust tract reconstruction. These methods are optimized for healthy brains, however, so perhaps they do not perform as well in damaged areas.

Our classifier was based on the fiber density of these connections. Prior studies report long-lasting differences in MD (mean diffusivity) and FA (fractional anisotropy) [15], so weighting the connectivity matrices using these diffusivity measures may increase accuracy, and may affect which tractography algorithm leads to the greatest classification accuracy. In future work, we will study this.

When we examined the connections contributing most to the classifier (those with the top 5% strongest weights), and we found connections spanning all lobes of the brain. Of these most-robust connections, there were more in the left hemisphere than in the right, and a number long-range, anterior-posterior connections. This could indicate that long-range connections are especially vulnerable to the disruptions caused by a traumatic brain injury. While our resolution for very short fibers is arguably less than that of long ones, this is an interesting possibility. It makes sense that long fibers would be more vulnerable, as they experience the acceleration-deceleration forces of TBI across a great length, and there is a greater probability that they contact an area of acute injury.

Our findings indicate that TBI, in the chronic phase, causes global disruption. Population studies in TBI are made difficult by the heterogeneity of the type, severity, and extent of the brain damage patients sustain. This spread from localized and presumably heterogeneous disruption into a global issue may occur through diaschisis. Diaschisis is the phenomenon whereby disruption of one injured brain area spreads to other connected brain areas. This is an on-going, longitudinal study, so we will have the opportunity to further investigate how disruption spreads, how recovery occurs, and how this is related to cognitive recovery.

5. REFERENCES

[1] Xu, J. et al., Diffuse axonal injury in severe traumatic brain injury visualized using high-resolution diffusion tensor imaging. **J Neurotrauma**, 24: 753-765.

[2] Giza, C.C. et al., *N*-methyl-*D*-aspartate receptor subunit changes after traumatic injury to the developing brain. **J Neurotrauma**, 23: 950-961, 2006.

[3] Desikan, R., et al., An automated labeling system for subdiving the human cerebral cortex on MRI scans into gyral based regions of interest. **NeuroImage**, 31: 968-980, 2006.

[4] Mori, S., et al., Three-dimensional tracking of axonal projections in the brain by magnetic resonance imaging. **Ann Neurol**, 45(2): 265-9, 1999.

[5] Basser, P.J., et al., In vivo fiber tractography using DT-MRI data. **Magn Reson Med**, 44(4): 625-32, 2000.

[6] Lazar, M., et al., White matter tractography using diffusion tensor deflection. **Hum Brain Mapp**, 18(4): 306-21, 2003.

[7] Aganj, I., et al., A Hough transform global probabilistic approach to multiple-subject diffusion MRI tractography. **Med Image Anal**, 15(4): 414-25, 2011.

[8] Parker, G.J., H.A. Haroon, and C.A. Wheeler-Kingshott, A framework for a streamline-based probabilistic index of connectivity (PICo) using a structural interpretation of MRI diffusion measurements. **J Magn Reson Imaging**, 18(2): 242-54, 2003.

[9] Wedeen, V.J. et al., The geometric structure of the brain fiber pathways. **Science**, 335: 1628-1634, 2012.

[10] Prasad, G. et al., Tractography Density and Network Measures in Alzheimer's Disease. **IEEE ISBI**, 692-695, 2013.

[10] Cortes, C. & Vapnik, V. Support-vector networks. **Machine Learn**, 20, 273-297, 1995.

[11] Kohavi, R. et al. A study of cross-validation and bootstrap for accuracy estimation and model selection. **Int Joint Conf on Artificial Intelligent**, 14: 1137-1145, 1995.

[12] Prasad, G. et al. Brain connectivity and novel network measures for Alzheimer's disease classification. **NBA**, *In Press.*

[13] De Martino, F. et al., Combining multivariate voxel selection and support vector machines for mapping classification for fMRI spatial patterns. **NeuroImage**, 43: 44-58, 2008.

[14] Wilde, E.A. et al., Diffusion tensor imaging in moderate-to-severe pediatric traumatic brain injury: changes within an 18 month post-injury interval. **Brain Imaging and Behavior**, 6: 404-416, 2012.

ACKNOWLEDGMENTS

This study was supported by the NICHDS (R01 HD061504). ELD, GP, LZ, and PT are also supported by NIH grants to PT: U54 EB020403 (BD2K), R01 EB008432, R01 AG040060, and R01 NS080655. CCG is supported by the UCLA BIRC, NS027544, NS05489, Child Neurology Foundation, and the Jonathan Drown Foundation. Scanning was supported by the Staglin IMHRO Center for Cognitive Neuroscience. We thank Alma Martinez and Alma Ramirez for their contributions to participant recruitment and study coordination; we also thank the participants and their families for contributing to the study.